

The mergegram of a dendrogram and its stability

Yury Elkin

Materials Innovation Factory and Computer Science department, University of Liverpool, UK
yura.elkin@gmail.com

Vitaliy Kurlin 

Materials Innovation Factory and Computer Science department, University of Liverpool, UK
vitaliy.kurlin@gmail.com

Abstract

This paper extends the key concept of persistence within Topological Data Analysis (TDA) in a new direction. TDA quantifies topological shapes hidden in unorganized data such as clouds of unordered points. In the 0-dimensional case the distance-based persistence is determined by a single-linkage (SL) clustering of a finite set in a metric space. Equivalently, the 0D persistence captures only edge-lengths of a Minimum Spanning Tree (MST). Both SL dendrogram and MST are unstable under perturbations of points. We define the new stable-under-noise mergegram, which outperforms previous isometry invariants on a classification of point clouds by PersLay.

2012 ACM Subject Classification Theory of computation → Computational geometry

Keywords and phrases clustering dendrogram, topological data analysis, persistence, stability

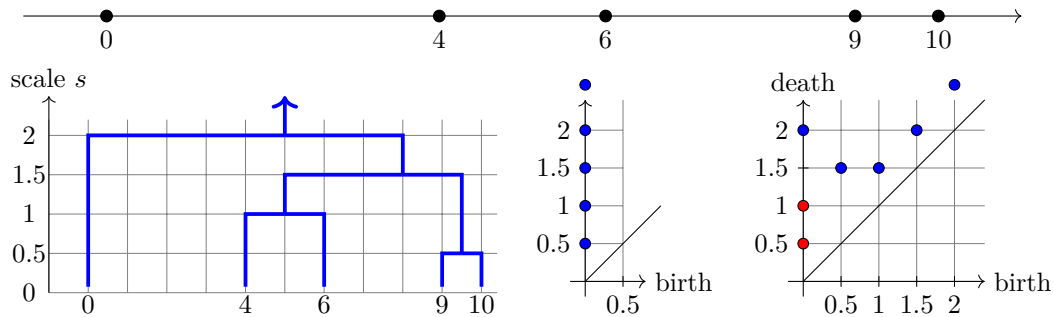
Digital Object Identifier 10.4230/LIPIcs.MFCS.2020.56

Funding The authors were supported by the £3.5M EPSRC grant EP/R018472/1 (2018-2023)

1 Introduction: motivations and overview of the new results

TDA is now expanding towards machine learning and statistics due to stability that was proved in a very general form by Chazal et al. [3]. The key idea of TDA is to view a given cloud of points across all scales s , e.g. by blurring given points to balls of a variable radius s . The resulting evolution of topological shapes is summarized by a persistence diagram.

► **Example 1.1.** Fig. 1 illustrates the key concepts (before formal definitions) for the point set $A = \{0, 4, 6, 9, 10\}$ in the real line \mathbb{R} . Imagine that we gradually blur original data points by growing balls of the same radius s around the given points. The balls of the closest points 9, 10 start overlapping at the scale $s = 0.5$ when these points merge into one cluster $\{9, 10\}$. This merger is shown by blue arcs joining at the node at $s = 0.5$ in the single-linkage dendrogram, see the bottom left picture in Fig. 1 and more details in Definition 2.1.



■ **Figure 1** **Top:** the 5-point cloud $A = \{0, 4, 6, 9, 10\} \subset \mathbb{R}$. **Bottom** from left to right: single-linkage dendrogram $\Delta_{SL}(A)$ from Definition 2.1, the 0D persistence diagram PD from Definition 4.4 and the new mergegram MG from Definition 3.4, where the red color shows dots of multiplicity 2.

The persistence diagram PD in the bottom middle picture of Fig. 1 represents this merger by the dot $(0, 0.5)$ meaning that a singleton cluster of (say) point 9 was born at the scale $s = 0$ and then died later at $s = 0.5$ (by merging into another cluster of point 10), see details in Definition 2.1. When two clusters $\{4, 6\}$ and $\{9, 10\}$ merge at $s = 1.5$, this event was previously encoded in the persistence diagram by the single dot $(0, 1.5)$ meaning that one cluster inherited from (say) point 10 was born at $s = 0$ and has died at $s = 1.5$.

For the same merger, the new mergegram in the bottom right picture of Fig. 1 associates the following two dots. The dot $(0.5, 1.5)$ means that the cluster $\{9, 10\}$ merged at the current scale $s = 1.5$ was previously formed at the smaller scale $s = 0.5$. The dot $(1, 1.5)$ means that another cluster $\{4, 6\}$ merged at the current scale $s = 1.5$ was formed at $s = 1$.

Every arc in the single-linkage dendrogram between nodes at scales b and d contributes one dot (b, d) to the mergegram, e.g. both singleton sets $\{9\}$, $\{10\}$ merging at $s = 0.5$ contribute two dots $(0, 0.5)$ or one dot of multiplicity 2 shown in red, see Fig. 1.

Example 1.1 shows that the mergegram MG retains more geometric information of a set A than the persistence diagram PD. It turns out that this new intermediate object (larger than PD and smaller than a full dendrogram) enjoys the stability of persistence, which makes MG useful for analysing noisy data in all cases when distance-based 0D persistence is used.

Here is the summary of new contributions to Topological Data Analysis.

- Definition 3.4 introduces the concept of a mergegram for any dendrogram of clustering.
- Theorem 5.3 and Example 5.4 justify that the mergegram of a single-linkage dendrogram is strictly stronger than the 0D persistence of a distance-based filtration of sublevel sets.
- Theorem 7.4 proves that the mergegram of any single-linkage dendrogram is stable in the bottleneck distance under perturbations of a finite set in the Hausdorff distance.
- Theorem 8.2 shows that the mergegram can be computed in a near linear time.

2 Related work on hierarchical clustering and deep neural networks

The aim of clustering is to split a given set of points into clusters such that points within one cluster are more similar to each other than points from different clusters.

A clustering problem can be made exact by specifying a distance between given points and restrictions on outputs, e.g. a number of clusters or a cost function to minimize.

All hierarchical clustering algorithms can output a hierarchy of clusters or a dendrogram visualising mergers of clusters as explained later in Definition 3.2. Here we introduce only the simplest single-linkage clustering, which plays the central role in the paper.

► **Definition 2.1** (single-linkage clustering). Let A be a finite set in a metric space X with a distance $d : X \times X \rightarrow [0, +\infty)$. Given a distance threshold, which will be called a scale s , any points $a, b \in A$ should belong to one *SL cluster* if and only if there is a finite sequence $a = a_1, \dots, a_m = b \in A$ such that any two successive points have a distance at most s , i.e. $d(a_i, a_{i+1}) \leq s$ for $i = 1, \dots, m - 1$. Let $\Delta_{SL}(A; s)$ denote the collection of SL clusters at the scale s . For $s = 0$, any point $a \in A$ forms a singleton cluster $\{a\}$. Representing each cluster from $\Delta_{SL}(A; s)$ over all $s \geq 0$ by one point, we get the *single-linkage dendrogram* $\Delta_{SL}(A)$ visualizing how clusters merge, see the first bottom picture in Fig. 1.1. ■

Another way to visualize SL clusters is to build a Minimum Spanning Tree below.

► **Definition 2.2** (Minimum Spanning Tree $MST(A)$). The *Minimum Spanning Tree* $MST(A)$ of a finite set A in a metric space X with a distance d is a tree (a connected graph without cycles) that has the vertex set A and the minimum total length of edges. We assume that the length of any edge between vertices $a, b \in A$ is measured as $d(a, b)$. ■

A review of the relevant past work on persistence diagrams is postponed to section 4, which introduces more auxiliary notions. A persistence diagram consists of dots $(b, d) \in \mathbb{R}^2$ whose birth/death coordinates represent a life interval $[b, d)$ of a homology class, e.g. a connected component in a Vietoris-Rips filtration, see the bottom middle picture in Fig. 1.

Persistence diagrams are isometry invariants that are stable under noise in the sense that a topological space and its noisy point sample have close persistence diagrams. This stability under noise allows us to classify continuous shapes by using only their discrete samples.

Imagine that several rigid shapes are sparsely represented by a few salient points, e.g. corners or local maxima of a distance function. Translations and rotations of these point clouds do not change the underlying shapes. Hence clouds should be classified modulo isometries that preserve distances between points. The important problem is to recognize of a shape, e.g. within a given set of representatives, from its sparse point sample with noise. This paper solves the problem by computing isometry invariants, namely the new mergegram, the 0D persistence and the pair-set of distances to two nearest neighbors for each point.

Since all dots in a persistence diagram are unordered, our experimental section 8 uses a neural network whose output is invariant under permutations of input point by construction. PersLay [2] is a collection of permutation invariant neural network layers i.e. functions on sets of points in \mathbb{R}^n that give the same output regardless of the order they are inserted.

PersLay extends the neural network layers introduced in Deep Sets [10]. PersLay introduces new layers to specially handle persistence diagrams, as well as new form of representing such layers. Each layer is a combination of a coefficient layer $\omega(p) : \mathbb{R}^n \rightarrow \mathbb{R}$, point transformation $\phi(p) : \mathbb{R}^n \rightarrow \mathbb{R}^q$ and permutation invariant layer op to retrieve the final output

$$\text{PersLay}(\text{diagram}) = \text{op}(\{\omega(p)\phi(p)\}), \text{ where } p \in \text{diagram (any set of points in } \mathbb{R}^n).$$

3 The merge module and mergegram of a dendrogram

The section introduces a merge module (a family of vector spaces with consistent linear maps) and a mergegram (a diagram of points in \mathbb{R}^2 representing a merge module).

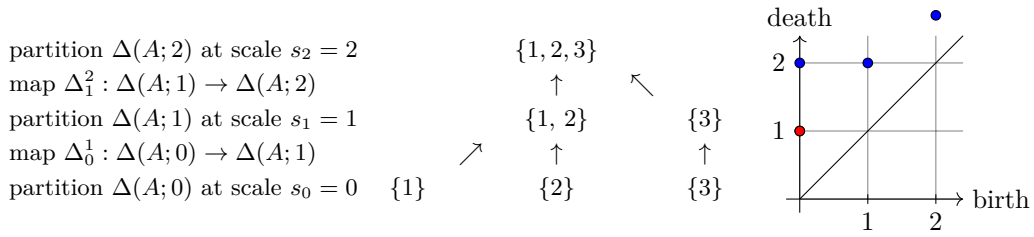
► **Definition 3.1** (partition set $\mathbb{P}(A)$). For any set A , a *partition* of A is a finite collection of non-empty disjoint subsets $A_1, \dots, A_k \subset A$ whose union is A . The *single-block* partition of A consists of the set A itself. The *partition set* $\mathbb{P}(A)$ consists of all partitions of A . ■

If $A = \{1, 2, 3\}$, then $(\{1, 2\}, \{3\})$ is a partition of A , but $(\{1\}, \{2\})$ and $(\{1, 2\}, \{1, 3\})$ are not. In this case the partition set $\mathbb{P}(A)$ consists of 5 partitions

$$(\{1\}, \{2\}, \{3\}), \quad (\{1, 2\}, \{3\}), \quad (\{1, 3\}, \{2\}), \quad (\{2, 3\}, \{1\}), \quad (\{1, 2, 3\}).$$

Definition 3.2 below extends the concept of a dendrogram from [1, section 3.1] to arbitrary (possibly, infinite) sets A . Since every partition of A is finite by Definition 3.1, we don't need to add that an initial partition of A is finite. Non-singleton sets are now allowed.

56:4 The mergegram of a dendrogram and its stability



■ **Figure 2** The dendrogram Δ on $A = \{1, 2, 3\}$ and its mergegram $MG(\Delta)$ from Definition 3.4.

► **Definition 3.2** (dendrogram of merge sets). A *dendrogram* over any set A is a function $\Delta : [0, \infty) \rightarrow \mathbb{P}(A)$ of a scale $s \geq 0$ satisfying the following conditions.

- (3.2a) There exists a scale $r \geq 0$ such that $\Delta(A; s)$ is the single block partition for all $s \geq r$.
- (3.2b) If $s \leq t$, then $\Delta(A; s)$ *refines* $\Delta(A; t)$, i.e. any set from $\Delta(s)$ is a subset of some set from $\Delta(t)$. These inclusions of subsets of X induce the natural map $\Delta_s^t : \Delta(s) \rightarrow \Delta(t)$.
- (3.2c) There are finitely many *merge scales* s_i such that

$$s_0 = 0 \text{ and } s_{i+1} = \sup\{s \mid \text{the map } \Delta_s^t \text{ is identity for } s' \in [s_i, s)\}, i = 0, \dots, m - 1.$$

Since $\Delta(A; s_i) \rightarrow \Delta(A; s_{i+1})$ is not an identity map, there is a subset $B \in \Delta(s_{i+1})$ whose preimage consists of at least two subsets from $\Delta(s_i)$. This subset $B \subset X$ is called a *merge set* and its *birth* scale is s_i . All sets of $\Delta(A; 0)$ are merge sets at the birth scale 0. The *life*(B) is the interval $[s_i, t)$ from its birth scale s_i to its *death* scale $t = \sup\{s \mid \Delta_{s_i}^s(B) = B\}$. ■

Dendrograms are usually represented as trees whose nodes correspond to all sets from the partitions $\Delta(A; s_i)$ at merge scales. Edges of such a tree connect any set $B \in \Delta(A; s_i)$ with its preimages under $\Delta(A; s_i) \rightarrow \Delta(A; s_{i+1})$. Fig. 2 shows the dendrogram on $A = \{1, 2, 3\}$.

In the dendrogram above, the partition $\Delta(A; 1)$ consists of $\{1, 2\}$ and $\{3\}$. The maps Δ_s^t induced by inclusions respect the compositions in the sense that $\Delta_s^t \circ \Delta_r^s = \Delta_r^t$ for any $r \leq s \leq t$, e.g. $\Delta_0^1(\{1\}) = \{1, 2\} = \Delta_0^1(\{2\})$ and $\Delta_0^1(\{3\}) = \{3\}$, i.e. Δ_0^1 is a well-defined map from the partition $\Delta(A; 0)$ in 3 singleton sets to $\Delta(A; 1)$, but isn't an identity.

At the scale $s_0 = 0$ the merge sets $\{1\}, \{2\}$ have *life* = $[0, 1)$, while the merge set $\{3\}$ has *life* = $[0, 2)$. At the scale $s_1 = 1$ the only merge set $\{1, 2\}$ has *life* = $[1, 2)$. At the scale $s_2 = 2$ the only merge set $\{1, 2, 3\}$ has *life* = $[2, +\infty)$. The notation Δ is motivated as the first (Greek) letter in the word dendrogram and by a Δ -shape of a typical tree above.

Condition (3.2a) means that a partition of X is trivial for all large scales s . Condition (3.2b) says that when the scale s is increasing sets from a partition $\Delta(s)$ can only merge with each other, but can not split. Condition (3.2c) implies that there are only finitely many mergers, when two or more subsets of X merge into a larger merge set.

► **Lemma 3.3** (single-linkage dendrogram). Given a metric space (X, d) and a finite set $A \subset X$, the single-linkage dendrogram $\Delta_{SL}(X)$ from Definition 2.1 satisfies Definition 3.2.

Proof. Since A is finite, there are only finitely many inter-point distances within A , which implies condition (3.2a,c). Let $f(p) : X \rightarrow \mathbb{R}$ be the distance from a point $p \in X$ to (the closest point of) A . Condition (3.2b) follows the inclusions $f^{-1}[0, s] \subseteq f^{-1}[0, t]$ for $s \leq t$. ◀

A *mergegram* represents lives of merge sets by dots with two coordinates (birth,death).

► **Definition 3.4** (mergegram $MG(\Delta)$). The mergegram of a dendrogram Δ from Definition 3.2 has the dot (birth,death) in \mathbb{R}^2 for each merge set A of Δ with $life(A)=[birth,death)$. If any life interval appears k times, the dot (birth,death) has the multiplicity k in $MG(\Delta)$. ■

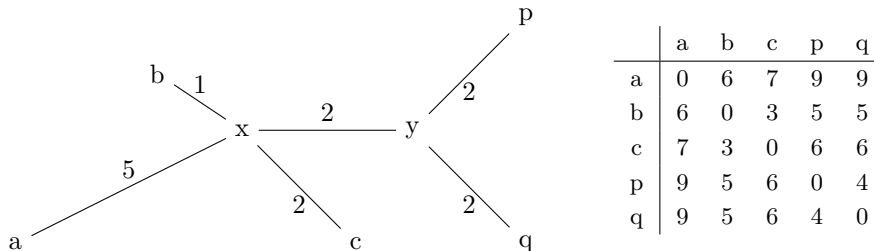
For simplicity, this paper considers vector spaces with coefficients (of linear combinations of vectors) only in $\mathbb{Z}_2 = \{0, 1\}$, which can be replaced by any field.

► **Definition 3.5** (merge module $M(\Delta)$). For any dendrogram Δ on a set X from Definition 3.2, the merge module $M(\Delta)$ consists of the vector spaces $M_s(\Delta)$, $s \in \mathbb{R}$, and linear maps $m_s^t : M_s(\Delta) \rightarrow M_t(\Delta)$, $s \leq t$. For any $s \in \mathbb{R}$ and $A \in \Delta(s)$, the space $M_s(\Delta)$ has the generator or a basis vector $[A] \in M_s(\Delta)$. For $s < t$ and any set $A \in \Delta(s)$, if the image of A under Δ_s^t coincides with $A \subset X$, i.e. $\Delta_s^t(A) = A$, then $m_s^t([A]) = [A]$, else $m_s^t([A]) = 0$. ■

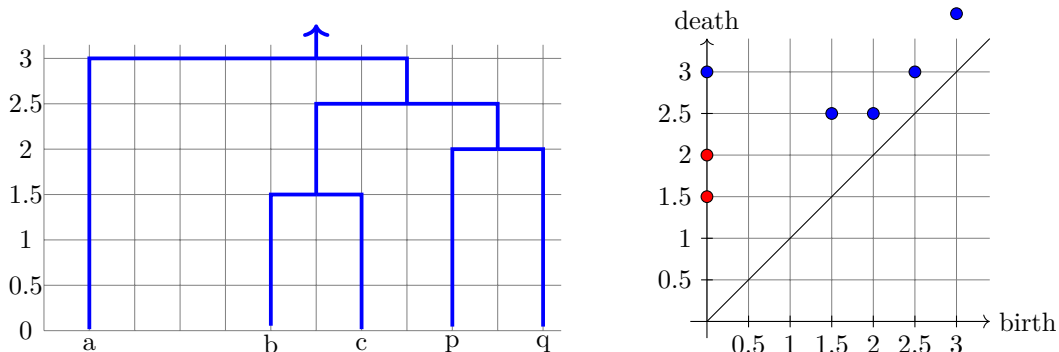
scale $s_3 = +\infty$		0		0	
map $m_2^{+\infty}$		↑		↑	
scale $s_2 = 2$		\mathbb{Z}_2	0	0	$\{\{1,2,3\}\}$
map m_1^2		↑	↑	↑	
scale $s_1 = 1$		$\mathbb{Z}_2 \oplus \mathbb{Z}_2$	0	0	$\{\{3\}\}$ $\{\{1,2\}\}$
map m_0^1		↑	↑	↑	
scale $s_0 = 0$		$\mathbb{Z}_2 \oplus \mathbb{Z}_2 \oplus \mathbb{Z}_2$	$\{\{1\}\}$	$\{\{2\}\}$	$\{\{3\}\}$

■ **Figure 3** The merge module $M(\Delta)$ of the dendrogram Δ on the set $X = \{1, 2, 3\}$ in Fig. 2.

► **Example 3.6.** Fig. 4 shows the metric space $X = \{a, b, c, d, e\}$ with distances defined by the shortest path metric induced by the specified edge-lengths, see the distance matrix.



■ **Figure 4** The set $X = \{a, b, c, d, e\}$ has the distance matrix defined by the shortest path metric.



■ **Figure 5** Left: the dendrogram Δ for the single linkage clustering of the set 5-point set $X = \{a, b, c, d, e\}$ in Fig. 4. Right: the mergegram $MG(\Delta)$, red dots have multiplicity 2.

The dendrogram Δ in the first picture of Fig. 5 generates the mergegram as follows:

- each of the singleton sets $\{b\}$ and $\{c\}$ has the dot $(0,1.5)$, so its multiplicity is 2;
- each of the singleton sets $\{p\}$ and $\{q\}$ has the dot $(0,2)$, so its multiplicity is 2;
- the singleton set $\{a\}$ has the dot $(0,3)$; the merge set $\{b, c\}$ has the dot $(1.5,2.5)$;
- the merge set $\{p, q\}$ has the dot $(2,2.5)$; the merge set $\{b, c, p, q\}$ has the dot $(2.5,3)$;
- the merge set $\{a, b, c, p, q\}$ has the dot $(3, +\infty)$.

4 Background on persistence modules and diagrams

This section introduces the key concepts from the thorough review by Chazal et al. [3]. As will become clear soon, the merge module of any dendrogram belongs to a wider class below.

► **Definition 4.1** (persistence module \mathbb{V}). A *persistence module* \mathbb{V} over the real numbers \mathbb{R} is a family of vector spaces V_t , $t \in \mathbb{R}$ with linear maps $v_s^t : V_s \rightarrow V_t$, $s \leq t$ such that v_t^t is the identity map on V_t and the composition is respected: $v_s^t \circ v_r^s = v_r^t$ for any $r \leq s \leq t$. ■

The set of real numbers can be considered as a category \mathbb{R} in the following sense. The objects of \mathbb{R} are all real numbers. Any two real numbers such that $a \leq b$ define a single morphism $a \rightarrow b$. The composition of morphisms $a \rightarrow b$ and $b \rightarrow c$ is the morphism $a \leq c$. In this language, a persistence module is a functor from \mathbb{R} to the category of vector spaces.

A basic example of \mathbb{V} is an interval module. An interval J between points $p < q$ in the line \mathbb{R} can be one of the following types: closed $[p, q]$, open (p, q) and half-open or half-closed $[p, q)$ and $(p, q]$. It is convenient to encode types of endpoints by \pm superscripts as follows:

$$[p^-, q^+] := [p, q], \quad [p^+, q^-] := (p, q), \quad [p^+, q^+] := [p, q], \quad [p^-, q^-] := (p, q).$$

The endpoints p, q can also take the infinite values $\pm\infty$, but without superscripts.

► **Example 4.2** (interval module $\mathbb{I}(J)$). For any interval $J \subset \mathbb{R}$, the *interval module* $\mathbb{I}(J)$ is the persistence module defined by the following vector spaces I_s and linear maps $i_s^t : I_s \rightarrow I_t$

$$I_s = \begin{cases} \mathbb{Z}_2, & \text{for } s \in J, \\ 0, & \text{otherwise;} \end{cases} \quad i_s^t = \begin{cases} \text{id}, & \text{for } s, t \in J, \\ 0, & \text{otherwise} \end{cases} \quad \text{for any } s \leq t.$$

The direct sum $\mathbb{W} = \mathbb{U} \oplus \mathbb{V}$ of persistence modules \mathbb{U}, \mathbb{V} is defined as the persistence module with the vector spaces $W_s = U_s \oplus V_s$ and linear maps $w_s^t = u_s^t \oplus v_s^t$.

We illustrate the abstract concepts above using geometric constructions of Topological Data Analysis. Let $f : X \rightarrow \mathbb{R}$ be a continuous function on a topological space. Its *sublevel* sets $X_s^f = f^{-1}((-\infty, s])$ form nested subspaces $X_s^f \subset X_t^f$ for any $s \leq t$. The inclusions of the sublevel sets respect compositions similarly to a dendrogram Δ in Definition 3.2.

On a metric space X with with a distance function $d : X \times X \rightarrow [0, +\infty)$, a typical example of a function $f : X \rightarrow \mathbb{R}$ is the distance to a finite set of points $A \subset X$. More specifically, for any point $p \in X$, let $f(p)$ be the distance from p to (a closest point of) A . For any $r \geq 0$, the preimage $X_r^f = f^{-1}((-\infty, r]) = \{q \in X \mid d(q, A) \leq r\}$ is the union of closed balls that have the radius r and centers at all points $p \in A$. For example, $X_0^f = f^{-1}((-\infty, 0]) = A$ and $X_{+\infty}^f = f^{-1}(\mathbb{R}) = X$.

If we consider any continuous function $f : X \rightarrow \mathbb{R}$, we have the inclusion $X_s^f \subset X_r^f$ for any $s \leq r$. Hence all sublevel sets X_s^f form a nested sequence of subspaces within X . The above construction of a *filtration* $\{X_s^f\}$ can be considered as a functor from \mathbb{R} to the category of topological spaces. Below we discuss the most practically used case of dimension 0.

► **Example 4.3** (persistent homology). For any topological space X , the 0-dimensional homology $H_0(X)$ is the vector space (with coefficients \mathbb{Z}_2) generated by all connected components of X . Let $\{X_s\}$ be any *filtration* of nested spaces, e.g. sublevel sets X_s^f based on a continuous function $f : X \rightarrow \mathbb{R}$. The inclusions $X_s \subset X_r$ for $s \leq r$ induce the linear maps between homology groups $H_0(X_s) \rightarrow H_0(X_r)$ and define the *persistent homology* $\{H_0(X_s)\}$, which satisfies the conditions of a persistence module from Definition 4.1. ■

If X is a finite set of m points, then $H_0(X)$ is the direct sum \mathbb{Z}_2^m of m copies of \mathbb{Z}_2 .

The persistence modules that can be decomposed as direct sums of interval modules can be described in a very simple combinatorial way by persistence diagrams of dots in \mathbb{R}^2 .

► **Definition 4.4** (persistence diagram $\text{PD}(\mathbb{V})$). Let a persistence module \mathbb{V} be decomposed as a direct sum of interval modules from Example 4.2 : $\mathbb{V} \cong \bigoplus_{l \in L} \mathbb{I}(p_l^*, q_l^*)$, where $*$ is $+$ or $-$. The *persistence diagram* $\text{PD}(\mathbb{V})$ is the multiset $\text{PD}(\mathbb{V}) = \{(p_l, q_l) \mid l \in L\} \setminus \{p = q\} \subset \mathbb{R}^2$. ■

The 0-dimensional persistent homology of a space X with a continuous function $f : X \rightarrow \mathbb{R}$ will be denoted by $\text{PD}\{H_0(X_s^f)\}$. Lemma 7.1 will prove that the merge module $M(\Delta)$ of any dendrogram Δ is also decomposable into interval modules. Hence the mergegram $\text{MG}(\Delta)$ from Definition 3.4 can be interpreted as the persistence diagram of the merge module $M(\Delta)$.

5 The mergegram is stronger than the 0-dimensional persistence

Let $f : X \rightarrow \mathbb{R}$ be the distance function to a finite subset A of a metric space (X, d) . The persistent homology $\{H_k(X_s^f)\}$ in any dimension k is invariant under isometries of X .

Moreover, the persistence diagrams of very different shapes, e.g. topological spaces and their discrete samples, can be easily compared by the bottleneck distance in Definition 6.3.

Practical applications of persistence are justified by Stability Theorem 6.4 saying that the persistence diagram continuously changes under perturbations of a given filtration or an initial point set. A similar stability of mergegrams will be proved in Theorem 7.4.

This section shows that the mergegram $\text{MG}(\Delta_{SL}(A))$ has more isometry information about the subset $A \subset X$ than the 0-dimensional persistent homology $\{H_0(X_s^f)\}$.

Theorem 5.3 shows how to obtain the 0D persistence $\text{PD}\{H_0(X_s^f)\}$ from $\text{MG}(\Delta_{SL}(A))$, where $f : X \rightarrow \mathbb{R}$ is the distance to a finite subset $A \subset X$. Example 5.4 builds two 4-point sets in \mathbb{R} whose persistence diagrams are identical, but their mergegrams are different.

We start from folklore Claims 5.1-5.2, which interpret the 0D persistence $\text{PD}\{H_0(X_s^f)\}$ using the classical concepts of the single-linkage dendrogram and Minimum Spanning Tree.

► **Claim 5.1** (0D persistence from Δ_{SL}). For a finite set A in a metric space (X, d) , let $f : X \rightarrow \mathbb{R}$ be the distance to A . In the single-linkage dendrogram $\Delta_{SL}(A)$, let $0 < s_1 < \dots < s_m < s_{m+1} = +\infty$ be all distinct merge scales. If $k \geq 2$ subsets of A merge into a larger subset of A at a scale s_i , the multiplicity of s_i is $\mu_i = k - 1$. Then the persistence diagram $\text{PD}\{H_0(X_s^f)\}$ consists of the dots $(0, s_i)$ with multiplicities μ_i , $i = 1, \dots, m + 1$. ■

► **Claim 5.2** (0D persistence from MST). For a set A of n points in a metric space (X, d) , let $f : X \rightarrow \mathbb{R}$ be the distance to A . Let a Minimum Spanning Tree $\text{MST}(A)$ have edge-lengths $l_1 \leq \dots \leq l_{n-1}$. The persistence diagram $\text{PD}\{H_0(X_s^f)\}$ consists of the $n - 1$ dots $(0, 0.5l_i)$ counted with multiplicities if some edge-lengths are equal, plus the infinite dot $(0, +\infty)$. ■

► **Theorem 5.3** (0D persistence from a mergegram). For a finite set A in a metric space (X, d) , let $f : X \rightarrow \mathbb{R}$ be the distance to A . Let the mergegram $\text{MG}(\Delta_{SL}(A))$ be a multiset $\{(b_i, d_i)\}_{i=1}^k$, where some dots can be repeated. Then the persistence diagram $\text{PD}\{H_0(X_s^f)\}$ is the difference of the multisets $\{(0, d_i)\}_{i=1}^k - \{(0, b_i)\}_{i=1}^k$ containing each dot $(0, s)$ exactly $\#b - \#d$ times, where $\#b$ is the number of births $b_i = s$, $\#d$ is the number of deaths $d_i = s$. All trivial dots $(0, 0)$ are ignored, alternatively we take $\{(0, d_i)\}_{i=1}^k$ only with $d_i > 0$. ■

Proof. In the language of Claim 5.1, let at a scale $s > 0$ of multiplicity μ exactly $\mu + 1$ subsets merge into a set $B \in \Delta_{SL}(A; s)$. By Claim 5.1 this set B contributes μ dots $(0, s)$ to the persistence diagrams $\text{PD}\{H_0(X_s^f)\}$. By Definition 3.4 the same set B contributes $\mu + 1$ dots of the form (b_i, s) , $i = 1, \dots, \mu + 1$, corresponding to the $\mu + 1$ sets that merge into B at the scale s . Moreover, the set B itself will merge later into a larger set, which creates one extra dot $(s, d) \in \text{PD}\{H_0(X_s^f)\}$. The exceptional case $B = A$ corresponds to $d = +\infty$.

If we remove one dot $(0, s)$ from the $\mu + 1$ dots counted above as expected in the difference $\{(0, d_i)\}_{i=1}^k - \{(0, b_i)\}_{i=1}^k$ of multisets, we get exactly μ dots $(0, s) \in \text{PD}\{H_0(X_s^f)\}$. The required formula has been proved for contributions of any merge set $B \subset A$. ◀

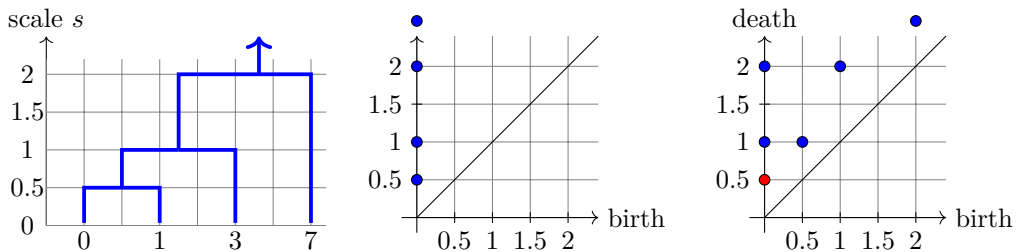
In Example 1.1 the mergegram in the last picture of Fig. 1 is the multiset of 9 dots:

$$\text{MG}(\Delta_{SL}(A)) = \{(0, 0.5), (0, 0.5), (0, 1), (0, 1), (0.5, 1.5), (1, 1.5), (0, 2), (1.5, 2), (2, +\infty)\}.$$

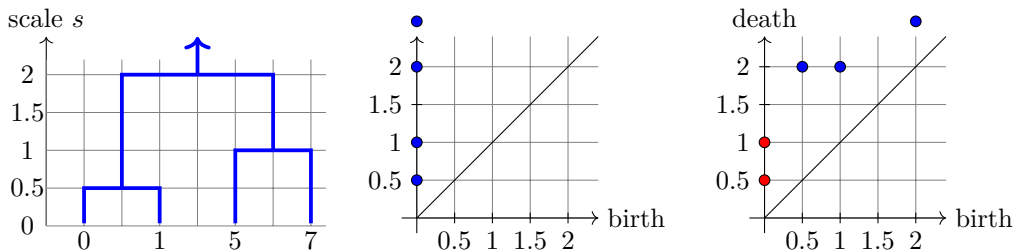
Taking the difference of multisets and ignoring trivial dots $(0, 0)$, we get

$$\text{PD}(H_0\{X_s^f\}) = \{(0, 0.5), (0, 0.5), (0, 1), (0, 1), (0, 1.5), (0, 1.5), (0, 2), (0, 2), (0, +\infty)\} - \{(0, 0.5), (0, 1), (0, 2)\} = \{(0, 0.5), (0, 1), (0, 1.5), (0, 2), (0, +\infty)\}$$
 as in Fig. 1.

► **Example 5.4** (the mergegram is stronger than 0D persistence). Fig. 6 and 7 show the dendrograms, identical 0D persistence diagrams and different mergegrams for the sets $A = \{0, 1, 3, 7\}$ and $B = \{0, 1, 5, 7\}$ in \mathbb{R} . This example together with Theorem 5.3 justify that the new mergegram is strictly stronger than 0D persistence as an isometry invariant.



■ **Figure 6** Left: single-linkage dendrogram $\Delta_{SL}(A)$ for $A = \{0, 1, 3, 7\} \subset \mathbb{R}$. Middle: the 0D persistence diagram for the sublevel filtration of the distance to A . Right: mergegram $\text{MG}(\Delta_{SL}(A))$.



■ **Figure 7** Left: single-linkage dendrogram $\Delta_{SL}(B)$ for $B = \{0, 1, 5, 7\} \subset \mathbb{R}$. Middle: the 0D persistence diagram for the sublevel filtration of the distance to B . Right: mergegram $\text{MG}(\Delta_{SL}(B))$.

6 Distances and stability of persistence modules

Definition 6.1 introduces homomorphisms between persistence modules, which are needed to state the stability of persistence diagrams $\text{PD}\{H_0(X_s^f)\}$ under perturbations of a function $f : X \rightarrow \mathbb{R}$. This result will imply a similar stability for the mergegram $\text{MG}(\Delta_{SL}(A))$ for the dendrogram $\Delta_{SL}(A)$ of the single-linkage clustering of a set A within a metric space X .

► **Definition 6.1** (a homomorphism of a degree δ between persistence modules). Let \mathbb{U} and \mathbb{V} be persistent modules over \mathbb{R} . A *homomorphism* $\mathbb{U} \rightarrow \mathbb{V}$ of degree $\delta \in \mathbb{R}$ is a collection of linear maps $\phi_t : U_t \rightarrow V_{t+\delta}$, $t \in \mathbb{R}$, such that the diagram commutes for all $s \leq t$.

$$\begin{array}{ccc} U_s & \xrightarrow{u_s^t} & U_t \\ \phi_s \downarrow & & \downarrow \phi_t \\ V_{s+\delta} & \xrightarrow{v_{s+\delta}^{t+\delta}} & V_{t+\delta} \end{array}$$

Let $\text{Hom}^\delta(\mathbb{U}, \mathbb{V})$ be all homomorphisms $\mathbb{U} \rightarrow \mathbb{V}$ of degree δ . Persistence modules \mathbb{U}, \mathbb{V} are *isomorphic* if they have inverse homomorphisms $\mathbb{U} \rightarrow \mathbb{V}$ and $\mathbb{V} \rightarrow \mathbb{U}$ of degree $\delta = 0$. ■

For a persistence module \mathbb{V} with maps $v_s^t : V_s \rightarrow V_t$, the simplest example of a homomorphism of a degree $\delta \geq 0$ is $1_{\mathbb{V}}^\delta : \mathbb{V} \rightarrow \mathbb{V}$ defined by the maps $v_{s+\delta}^{s+\delta}$, $t \in \mathbb{R}$. So the maps v_s^t defining the structure of \mathbb{V} shift all vector spaces V_s the difference of scale $\delta = t - s$.

The concept of interleaved modules below is an algebraic generalization of a geometric perturbation of a set X in terms of (the homology of) its sublevel sets X_s .

► **Definition 6.2** (interleaving distance ID). Persistent modules \mathbb{U} and \mathbb{V} are δ -interleaved if there are homomorphisms $\phi \in \text{Hom}^\delta(\mathbb{U}, \mathbb{V})$ and $\psi \in \text{Hom}^\delta(\mathbb{V}, \mathbb{U})$ such that $\phi \circ \psi = 1_{\mathbb{V}}^{2\delta}$ and $\psi \circ \phi = 1_{\mathbb{U}}^{2\delta}$. The *interleaving distance* is $\text{ID}(\mathbb{U}, \mathbb{V}) = \inf\{\delta \geq 0 \mid \mathbb{U} \text{ and } \mathbb{V} \text{ are } \delta\text{-interleaved}\}$. ■

If $f, g : X \rightarrow \mathbb{R}$ are continuous functions such that $\|f - g\|_\infty \leq \delta$ in the L_∞ -distance, the persistence modules $H_k\{f^{-1}(-\infty, s]\}$, $H_k\{g^{-1}(-\infty, s]\}$ are δ -interleaved for any k [4]. The last conclusion extended to persistence diagrams in terms of the bottleneck distance below.

► **Definition 6.3** (bottleneck distance BD). Let multisets C, D contain finitely many points $(p, q) \in \mathbb{R}^2$, $p < q$, of finite multiplicity and all diagonal points $(p, p) \in \mathbb{R}^2$ of infinite multiplicity. For $\delta \geq 0$, a δ -matching is a bijection $h : C \rightarrow D$ such that $|h(a) - a|_\infty \leq \delta$ in the L_∞ -distance on the plane for any point $a \in C$. The *bottleneck distance* between persistence modules \mathbb{U}, \mathbb{V} is $\text{BD}(\mathbb{U}, \mathbb{V}) = \inf\{\delta \mid \text{there is a } \delta\text{-matching between } \text{PD}(\mathbb{U}) \text{ and } \text{PD}(\mathbb{V})\}$. ■

The original stability of persistence for sequences of sublevel sets persistence was extended as Theorem 6.4 to q -tame persistence modules. Intuitively, a persistence module \mathbb{V} is q -tame any non-diagonal square in the persistence diagram $\text{PD}(\mathbb{V})$ contains only finitely many of points, see [3, section 2.8]. Any finitely decomposable persistence module is q -tame.

► **Theorem 6.4** (stability of persistence modules). [3, isometry theorem 4.11] Let \mathbb{U} and \mathbb{V} be q -tame persistence modules. Then $\text{ID}(\mathbb{U}, \mathbb{V}) = \text{BD}(\text{PD}(\mathbb{U}), \text{PD}(\mathbb{V}))$, where ID is the interleaving distance, BD is the bottleneck distance between persistence modules. ■

7 Stability of the mergegram for any single-linkage dendrogram

In a dendrogram Δ from Definition 3.2, any merge set A of Δ has a life interval $\text{life}(A) = [b, d)$ from its birth scale b to its death scale d . Lemmas 7.1 and 7.3 are proved in appendices.

► **Lemma 7.1** (merge module decomposition). For any dendrogram Δ in the sense of Definition 3.2, the merge module $M(\Delta) \cong \bigoplus_A \mathbb{I}(\text{life}(A))$ decomposes over all merge sets A . ■

Lemma 7.1 will allow us to use the stability of persistence in Theorem 6.4 for merge modules and also Lemma 7.3. Stability of the mergegram $\text{MG}(\Delta_{SL}(A))$ will be proved under perturbations of A in the Hausdorff distance defined below.

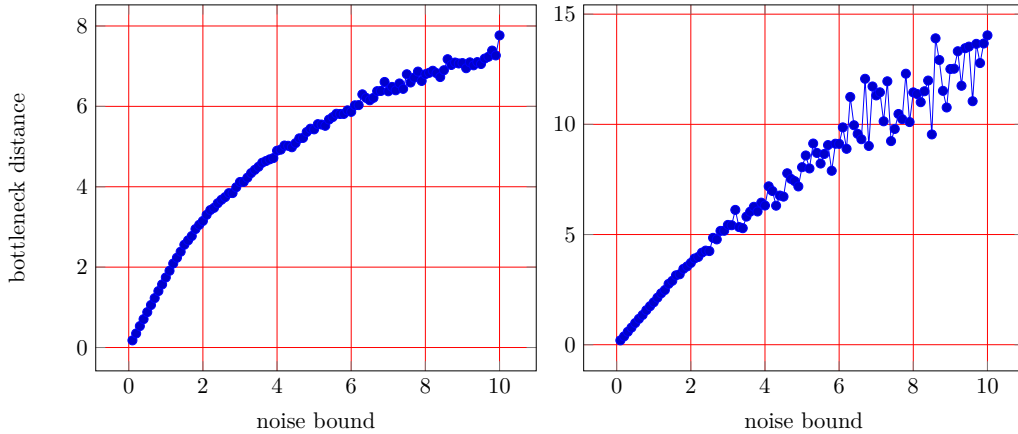
► **Definition 7.2** (Hausdorff distance HD). For any subsets A, B of a metric space (X, d) , the Hausdorff distance $\text{HD}(A, B)$ is $\max\{\sup_{a \in A} \inf_{b \in B} d(a, b), \sup_{b \in B} \inf_{a \in A} d(a, b)\}$. ■

► **Lemma 7.3** (merge modules interleaved). If any subsets A, B of a metric space (X, d) have $\text{HD}(A, B) = \delta$, then the merge modules $M(\Delta_{SL}(A))$ and $M(\Delta_{SL}(B))$ are δ -interleaved. ■

► **Theorem 7.4** (stability of a mergegram). Any finite subsets A, B of a metric space (X, d) have the mergegrams $\text{BD}(\text{MG}(\Delta_{SL}(A)), \text{MG}(\Delta_{SL}(B))) \leq \text{HD}(A, B)$. Hence any small perturbation of A in the Hausdorff distance yields a similarly small perturbation in the bottleneck distance for its mergegram $\text{MG}(\Delta_{SL}(A))$ of the single-linkage clustering dendrogram $\Delta_{SL}(A)$.

Proof. The given subsets A, B with $\text{HD}(A, B) = \delta$ have δ -interleaved merge modules by Lemma 7.3, i.e. $\text{ID}(\text{MG}(\Delta_{SL}(A)), \text{MG}(\Delta_{SL}(B))) \leq \delta$. Since any merge module $M(\Delta)$ is finitely decomposable, hence q -tame, by Lemma 7.1, the corresponding mergegram $\text{MG}(M(\Delta))$ satisfies Theorem 6.4, i.e. $\text{BD}(\text{MG}(\Delta_{SL}(A)), \text{MG}(\Delta_{SL}(B))) \leq \delta$ as required. ◀

Theorem 7.4 is confirmed by the following experiment on cloud perturbations in Fig. 8.



■ **Figure 8** The bottleneck distances (average on the left, maximum on the right) between mergegrams of sampled point clouds and their perturbations. Both graphs are below the line $y = 2x$.

1. We uniformly generate $N = 100$ black points in the cube $[0, 100]^3 \subset \mathbb{R}^3$.
2. Then we generate a random number of red points such that the ϵ ball of every black point randomly has 1, 2 or 3 red points for a noise bound $\epsilon \in [0.1, 10]$ taken with a step size 0.1.
3. Compute the bottleneck distance between the mergegrams of black and red points.
4. Repeat the experiment $K = 100$ times, plot the average and maximum in Fig. 8.

8 Experiments on a classification of point sets and conclusions

Algorithm 8.1 computes the mergegram of the SL dendrogram for any finite set $A \subset \mathbb{R}^m$.

► Algorithm 8.1.

Input : a finite point cloud $A \subset \mathbb{R}^m$

Compute $\text{MST}(A)$ and sort all edges of $\text{MST}(A)$ in increasing order of length

Initialize Union-Find structure U over A . Set all points of A to be their components.

Initialize the function $\text{prev}: \text{Components}[U] \rightarrow \mathbb{R}$ by setting $\text{prev}(t) = 0$ for all t

Initialize the vector **Output** that will consists of pairs in $\mathbb{R} \times \mathbb{R}$

for Edge $e = (a, b)$ in the set of edges (increasing order) **do**

 Find components c_1 and c_2 of a and b respectively in Union-Find U

 Add pairs $(\text{prev}[c_1], \text{length}(e)), (\text{prev}[c_2], \text{length}(e)) \in \mathbb{R}^2$ to **Output**

 Merge components c_1 and c_2 in Union-Find U and denote the component by t

 Set $\text{prev}[t] = \text{length}(e)$

end for

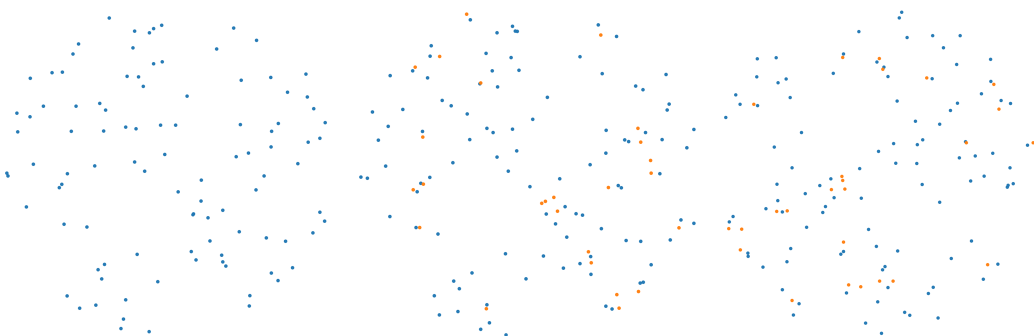
return **Output**

Let $\alpha(n)$ be the inverse Ackermann function. Other constants below are defined in [9].

► **Theorem 8.2** (a fast mergegram computation). For any cloud $A \subset \mathbb{R}^m$ of n points, the mergegram $\text{MG}(\Delta_{SL}(A))$ can be computed in time $O(\max\{c^6, c_p^2 c_l^2\} c^{10} n \log n \alpha(n))$.

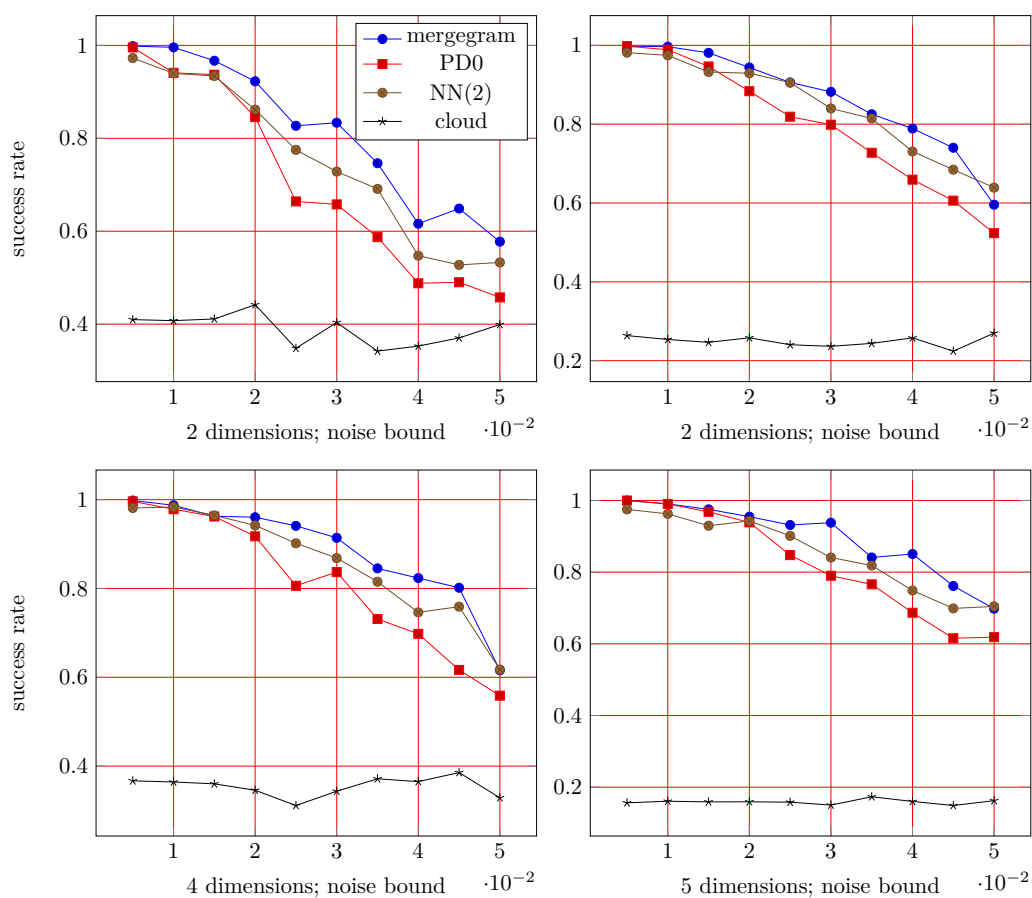
Proof. A Minimum Spanning Tree $\text{MST}(A)$ needs $O(\max\{c^6, c_p^2 c_l^2\} c^{10} n \log n \alpha(n))$ time by [9, Theorem 5.1]. The rest of Algorithm 8.1 is dominated by $O(n\alpha(n))$ Union-Find operations. Hence the full algorithm has the same computational complexity as the MST. ◀

The experiments summarized in Fig. 10 show that the mergegram curve in blue outperforms other isometry invariants on the isometry classification by the state-of-the-art PersLay. We generated 10 classes of 100-point clouds within the unit ball \mathbb{R}^m for $m = 2, 3, 4, 5$. For each class, we made 100 copies of each cloud and perturbed every point by a uniform random shift in a cube of the size $2 \times \epsilon$, where ϵ is called a *noise bound*. For each of 100 perturbed clouds, we added 25 points such that every new point is ϵ -close to an original point. Within each of 10 classes all 100 clouds were randomly rotated within the unit ball around the origin, see Fig. 9. For each of the resulting 1000 clouds, we computed the mergegram, 0D persistence diagram and the diagram of pairs of distances to two nearest neighbors for every point.



■ **Figure 9** **Left**: an initial random cloud with 100 blue points. **Middle**: all blue points are perturbed, 25 extra orange points are added. **Right**: a cloud is rotated through a random angle. Can we recognize that the initial and final clouds are in the same isometry class modulo small noise?

56:12 The mergegram of a dendrogram and its stability



■ **Figure 10** Success rates of PersLay in identifying isometry classes of 100-point clouds uniformly sampled in a unit ball, averaged over 5 different clouds and 5 cross-validations with 20/80 splits.

The machine learning part has used the obtained diagrams as the input-data for the Perslay [2]. Each dataset was split into learning and test subsets in ratio 4:1. The learning loops ran by iterating over mini-batches consisting of 128 elements and going through the full dataset for a given number of epochs. The success rate was measured on the test subset.

The original Perslay module was rewritten in Tensorflow v2 and RTX 2080 graphics card was used to run the experiments. The technical concepts of PersLay are explained in [2]:

- Adam(Epochs = 300, Learning rate = 0.01)
- Coefficients = Linear coefficients
- Functional layer = [PeL(dim=50), PeL(dim=50, operationalLayer=PermutationMaxLayer)].
- Operation layer = TopK(50)

The PersLay training has used the following invariants compared in Fig. 10:

- cloud : the initial cloud A of points corresponds to the baseline curve in black;
- PD0: the 0D persistence diagram PD for distance-based filtrations of sublevel sets in red;
- NN(2) brown curve: for each point $a \in A$ includes distances to two nearest neighbors;
- the mergegram $MG(\Delta_{SL}(A))$ of the SL dendrogram has the blue curve above others.

Fig. 10 shows that the new mergegram has outperformed all other invariants on the isometry classification problem. The 0D persistence turned out to be weaker than the

pairs of distances to two neighbors. The topological persistence has found applications in data skeletonization with theoretical guarantees [8, 5]. We are planning to extend the experiments in section 8 for classifying rigid shapes by combining the new mergegram with the 1D persistence, which has the fast $O(n \log n)$ time for any 2D cloud of n points [7, 6].

In conclusion, the paper has extended the 0D persistence to a stronger isometry invariant, which has kept the celebrated stability under noise important for applications to noisy data. The initial C++ code for the mergegram is at <https://github.com/YuryUoL/Mergegram> and will be updated. We thank all the reviewers for their valuable time and helpful suggestions.

References

- 1 Gunnar Carlsson and Facundo Memoli. Characterization, stability and convergence of hierarchical clustering methods. *Journal of machine learning research*, 11:1425–1470, 2010.
- 2 Mathieu Carriere, Frederic Chazal, Yuichi Ike, Theo Lacombe, Martin Royer, and Yuhei Umeda. Perslay: A neural network layer for persistence diagrams and new graph topological signatures. *AISTATS*, *arXiv:1904.09378*, 2020.
- 3 Frédéric Chazal, Vin De Silva, Marc Glisse, and Steve Oudot. *The structure and stability of persistence modules*. Springer, 2016.
- 4 David Cohen-Steiner, Herbert Edelsbrunner, and John Harer. Stability of persistence diagrams. *Discrete & Computational Geometry*, 37(1):103–120, 2007.
- 5 Sara Kalisnik, Vitaliy Kurlin, and Davorin Lesnik. A higher-dimensional homologically persistent skeleton. *Adv. App. Maths*, 102:113–142, 2019.
- 6 Vitaliy Kurlin. Auto-completion of contours in sketches, maps and sparse 2d images based on topological persistence. In *Proceedings of SYNASC 2014 workshop CTIC: Computational Topology in Image Context*, pages 594–601. IEEE, 2014.
- 7 Vitaliy Kurlin. A fast and robust algorithm to count topologically persistent holes in noisy clouds. In *Proceedings of the IEEE Conference on Computer Vision and Pattern Recognition*, pages 1458–1463, 2014.
- 8 Vitaliy Kurlin. A homologically persistent skeleton is a fast and robust descriptor of interest points in 2d images. In *LNCS, Proceedings of CAIP: Computer Analysis of Images and Patterns*, volume 9256, pages 606 – 617, 2015.
- 9 William B March, Parikshit Ram, and Alexander G Gray. Fast euclidean minimum spanning tree: algorithm, analysis, and applications. In *Proceedings of SIG KDD: Knowledge discovery and data mining*, pages 603–612, 2010.
- 10 Manzil Zaheer, Satwik Kottur, Siamak Ravanbakhsh, Barnabas Poczos, Russ R Salakhutdinov, and Alexander J Smola. Deep sets. In *Advances in neural information processing systems*, pages 3391–3401, 2017.